

AVIRIS DATA CHARACTERISTICS AND THEIR EFFECTS ON SPECTRAL
DISCRIMINATION OF ROCKS EXPOSED IN THE DRUM MOUNTAINS, UTAH: RESULTS
OF A PRELIMINARY STUDY

G. B. BAILEY, U.S. Geological Survey, EROS Data Center, Sioux Falls,
South Dakota, U.S.A.; J. L. DWYER, TGS Technology, Inc.*, EROS Data
Center, Sioux Falls, South Dakota, U.S.A.; and D. J. MEYER, TGS
Technology, Inc.*, EROS Data Center, Sioux Falls, South Dakota, U.S.A.

ABSTRACT

Airborne Visible and Infrared Imaging Spectrometer (AVIRIS) data collected over a geologically diverse field site and over a nearby calibration site were analyzed and interpreted in efforts to document radiometric and geometric characteristics of AVIRIS, quantify and correct for detrimental sensor phenomena, and evaluate the utility of AVIRIS data for discriminating rock types and identifying their constituent mineralogy. AVIRIS data acquired for these studies exhibit a variety of detrimental artifacts and have lower signal-to-noise ratios than expected in the longer wavelength bands. Artifacts are both inherent in the image data and introduced during ground processing, but most may be corrected by appropriate processing techniques. Poor signal-to-noise characteristics of this AVIRIS data set limited the usefulness of the data for lithologic discrimination and mineral identification. Various data calibration techniques, based on field-acquired spectral measurements, were applied to the AVIRIS data. Major absorption features of hydroxyl-bearing minerals were resolved in the spectra of the calibrated AVIRIS data, and the presence of hydroxyl-bearing minerals at the corresponding ground locations was confirmed by field data.

INTRODUCTION

The Airborne Visible and Infrared Imaging Spectrometer (AVIRIS) is potentially a powerful earth remote sensing tool, and it may provide geologists with their most effective capability yet to map

Publication authorized by the Director, U.S. Geological Survey.

Any use of trade names and trademarks in this publication is for descriptive purposes only and does not constitute endorsement by the U.S. Geological Survey.

* Work performed under U.S. Geological Survey contract
14-08-0001-22521.

lithologic variation and determine rock composition from remotely sensed data. However, in order for AVIRIS data to be applied most successfully in the solution of geologic and other interdisciplinary scientific problems, a variety of instrument and data characteristics must first be determined and evaluated. The radiometry and geometry of AVIRIS data must be characterized, and the information content of the data relative to specific interdisciplinary measurement requirements must be determined.

OBJECTIVES

The overall goal of these studies was to use the attributes of the selected field sites to determine and evaluate as many characteristics and capabilities of AVIRIS as possible, particularly as relate to geologic applications of AVIRIS data. Specific objectives identified at the outset were to:

- evaluate radiometric fidelity and spectral resolution
- document geometric characteristics
- quantify detrimental sensor phenomena
- evaluate capabilities to identify constituent mineralogy of diverse rock types
- evaluate effects of vegetation on such capabilities
- develop improved data products for interpretation

FIELD SITE CHARACTERISTICS

The Drum Mountains in west-central Utah were selected as the primary field site for these studies because good exposures of many diverse rock and alteration types present in an area of about 25 square km make the site particularly well suited for geologic evaluation of AVIRIS data. Furthermore, the detailed geology of the area is well documented (Bailey, 1974; Lindsay, 1979), and there exists a variety of other remotely sensed and ground-based data that also contribute to a comprehensive evaluation of AVIRIS data (Bailey and others, 1985).

Rocks exposed in the field area include a thick sequence of west-dipping Cambrian limestones, dolomites, and shales that overlies an even thicker, heterogeneous sequence of Cambrian and pre-Cambrian quartzite and argillite. Intermediate to silicic Tertiary volcanic rocks occur in fault contact with the sedimentary rocks in the northern part of the area, and older intermediate to mafic Tertiary volcanic rocks overlie the sediments on the west and south. The volcanic rocks have been hydrothermally altered in places, and some carbonate rocks adjacent to the volcanics have been bleached and recrystallized. A contact metamorphic aureole, which is characterized by development of calcsilicate mineralization in limestone and shale units, occurs in the central part of the area. The aureole is associated with the intrusion of two small stocks. One of the intrusives is a diorite and is essentially unaltered where exposed. The other was probably a monzonite, but it has undergone such intense hydrothermal alteration that the original lithology is uncertain.

A second field site, located near Pavant Butte and approximately 50 km south of the primary site, was used for data calibration purposes. It is characterized by rather large, uniform, and topographically flat occurrences of black volcanic soils, light buff-colored dry lake sediments, and white salt crusts.

APPROACH TO DATA ANALYSIS AND INTERPRETATION

Data Acquisition

AVIRIS data were acquired over the two field sites near solar noon on September 18, 1987, under cloud-free, low-haze atmospheric conditions. The data swath collected over the calibration site was almost precisely that which was requested, but a deviation of approximately 3 km over the primary site resulted in the exclusion of geologic targets in the thick basal quartzite and argillite units.

Concurrent with the AVIRIS flyover, ground spectral measurements of the light, intermediate, and dark targets at the Pavant Butte calibration site were collected using a Geophysical Environmental Research, Inc. (GER) Infra-Red Intelligent Spectroradiometer (IRIS). Field spectra of various rock and soil targets in the primary Drum Mountains field site were collected using an IRIS on the two days prior to the AVIRIS flyover. In addition, an extensive set of ground spectral data, including nearly all rock and alteration units in the primary field site, was acquired during the first week in August 1988 using an IRIS and the Portable Instantaneous Display and Analysis Spectrometer (PIDAS). Selected field stations flagged in August were reacquired in September as a mechanism for relating data collected during the two different collection efforts. Surface soil moisture conditions appeared to be uniformly dry with the possible exception of a small number of sites measured the day after a thunderstorm that occurred during the August field effort. However, effects of this possible variation are not evident in the data.

Image Quality Analysis and Artifact Correction

Preliminary analysis of this AVIRIS data set revealed a variety of detrimental data artifacts and noise, as well as a lower signal-to-noise ratio than expected in some of the data. Consequently, initial efforts were devoted to identifying and correcting artifacts that would hamper data analysis and interpretation. These artifacts are of two types: those that are inherent in the AVIRIS flight data, and those that are introduced during subsequent processing of the flight data. The inherent artifacts are line drops, low output signal for individual bands, and coherent (periodic) noises. Processing artifacts originate from noises in dark current data used during calibration and from spectral resampling that is performed to produce contiguous and evenly incremented wavelength bands from the original bands that overlap and have varying bandwidths.

The line drops and low output bands in the image data were corrected by straightforward means. Bad line segments were replaced by averaging adjacent lines, and low output bands were replaced by averaging adjacent bands. Table 1 lists the AVIRIS bands with low output, as determined by observing dark current levels.

Coherent noise patterns were the most apparent artifacts in the image data. Initially, one band from each spectrometer (fig. 1) was analyzed to determine the frequency and magnitude of these noises. Due to the prominence of noise in spectrometers B and D, detailed Fourier analysis then was performed on 32 bands from both the B and D spectrometers. Each band was transformed individually, and the resulting magnitudes were averaged for each 32-band subset and used to locate noise frequencies (figs. 2a and 2b). The following observations were made:

- (1) All components of the coherent noises occur at very specific horizontal frequencies.
- (2) Many noise patterns appear to be invariant with respect to spectrometer, and with respect to channel within a spectrometer.
- (3) The frequency components of the noise can be categorized as belonging to one of two groups. The first group is invariant with respect to vertical frequency, appearing as a modulation between horizontally adjacent pixels. Components of the second noise group exhibit well-defined horizontal harmonic relationships and a weak time-dependent preference for certain vertical frequencies. These components interact to produce the "herringbone" pattern seen in the image data.

Table 1. Low output AVIRIS bands.

Raw channel #	Spectrometer	Raw channel #	Spectrometer
20	A	162 *	D
24	A	163 *	D
26	A	165 *	D
28	A	168	D
32 *	A	169	D
34 *	B	173	D
40	B	176	D
64	B	189	D
72	B	205	D
80	B		

* Indicates redundant channel due to spectrometer overlap.

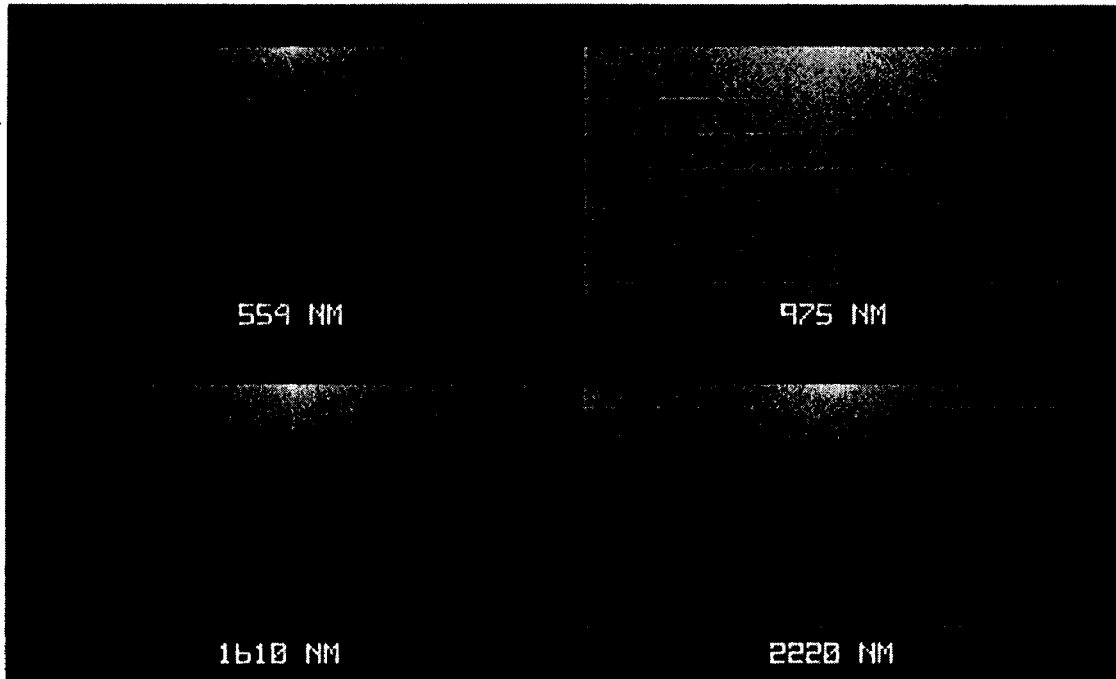


Fig. 1. Log_{10} magnitudes of sample bands from each of the four AVIRIS spectrometers. DC is centered at the top. Vertical axes correspond to horizontal frequencies (0 to 0.5 cycles/sample), and horizontal axes correspond to vertical frequencies (-0.5 to 0.5 cycles/line).

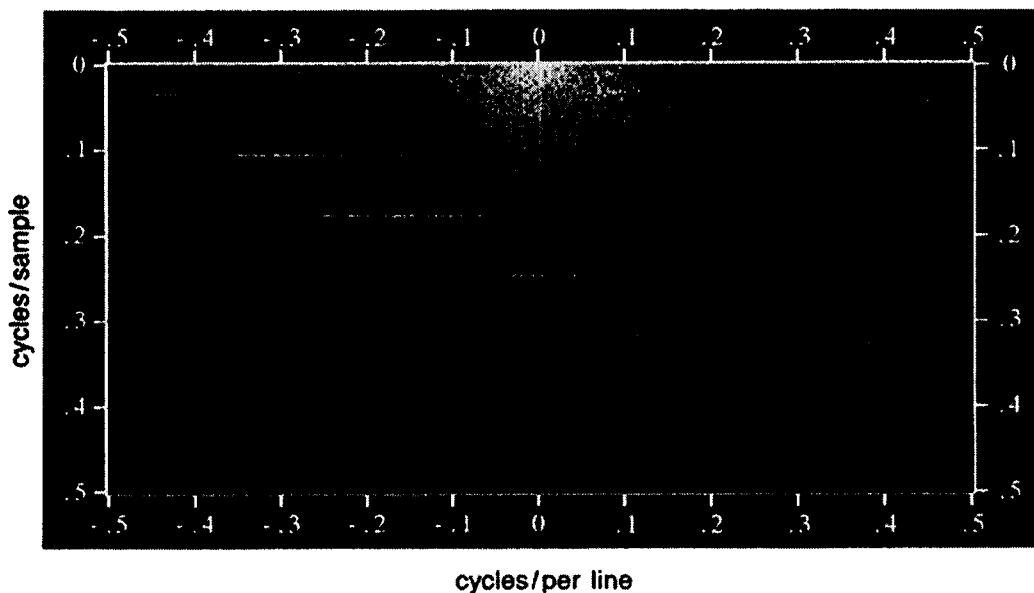


Fig. 2a. Log_{10} of the average magnitude of 32 consecutive bands from spectrometer B (0.71 to 1.00 micrometers). Horizontal frequencies are plotted vertically, and vertical frequencies are plotted horizontally.

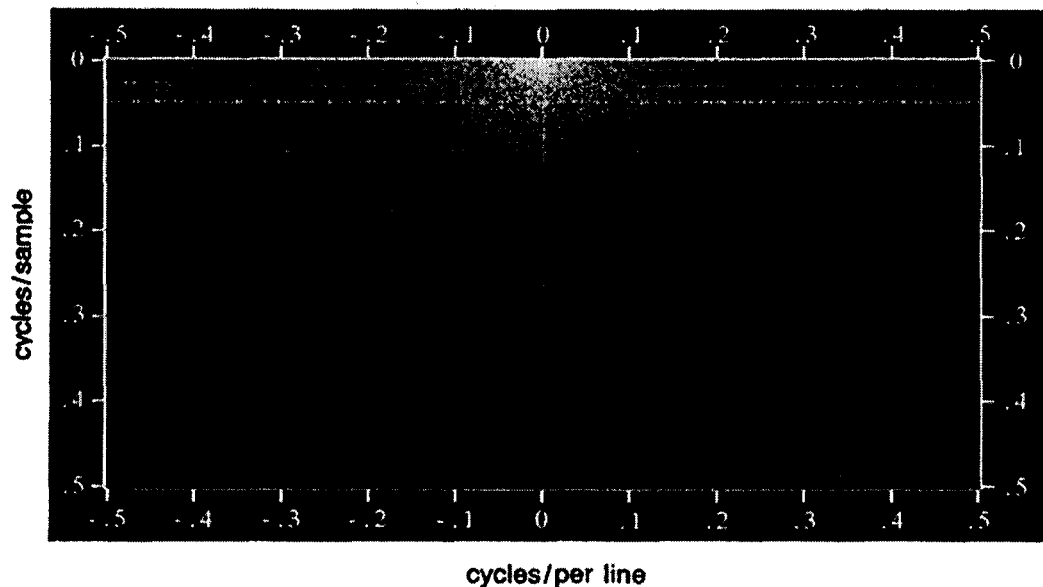


Fig. 2b. \log_{10} of the average magnitude of 32 consecutive bands from spectrometer D (2.11 to 2.41 micrometers). Horizontal frequencies are plotted vertically, and vertical frequencies are plotted horizontally.

Some of the major noise components were removed from the data by using "Gaussian notch" frequency filters (Moik, 1980). Table 2 is a list of noise frequencies having the characteristics of the first noise group, and table 3 lists those belonging to the second group.

Spectral resampling of AVIRIS images introduces a "smearing" of information between adjacent bands. This is particularly troublesome when low output bands are present in the data, because the resampling process causes these bands to corrupt immediately adjacent bands. To avoid this source of data degradation, raw AVIRIS data used in data analysis were processed without spectral resampling.

A final source of degradation is the subtraction of dark current data from the image data. The dark current data themselves were quite noisy, and the dark current noise from spectrometer B exhibited a pronounced periodicity with components at 0.11, 0.29, 0.31 and 0.42 cycles/line. Consequently, these data were smoothed by a moving 101-element averaging filter (Reimer and others, 1987). This smoothing did not, however, take into account offset discontinuities (Vane, 1987a). For the Drum Mountains data, the locations of these discontinuities were visually identified, and the dark current data were smoothed between these locations only.

The characteristics of "total noise" (not attempting to differentiate between systematic and random noises) were determined by measuring the standard deviation of the image over a uniformly bright and topographically flat hardpan target and over a nearby lake.

Figure 3 plots these measurements for both targets. Three points can be made about this figure. First, the major influences (assumed to be system noise) on the standard deviation appear to be purely additive; no significant dependence on target brightness is evident.

Table 2. Periodic noise components that are invariant with vertical frequency.

Horizontal frequency (cyc/samp)	Spectrometer	Horizontal frequency (cyc/samp)	Spectrometer
0.010 *	B,D	0.361	B
.030 *	B,D	.369	D
.043	B	.383	B
.049 *	B,D	.387	B,D
.064	B	.402	B
.148	D	.408	D
.168	D	.412	B,D
.201	B	.430	D
.209	D	.457	D
.214	B,D	.468	B,D
.250	B	.477 *	A,B,C,D +
.289	B	.480 *	D
.305	B	.484	B
.320	B	.486 *	B,D

* Indicates prominent noise feature.

+ Figures for A and C spectrometers were determined from bands at 0.554 and 1.61 micrometers, respectively.

Table 3. Periodic noise components exhibiting vertical frequency dependence.

Horizontal frequency (cyc/samp)	Vertical peak frequency (spec. B) (cyc/line)	Vertical peak frequency (spec. D) (cyc/line)
0.004	0.094	----
.016	.277	----
.018	.461	----
.025	.469	-0.457
.035 *	.434	- .429
.105 *	.295	- .295
.176 *	.164	- .174
.246 *	.029	- .033
.316 *	.113	.113
.326 +	.459	

* Indicates element of harmonic sequence (all spectrometers).

+ Possible aliased element of harmonic sequence.

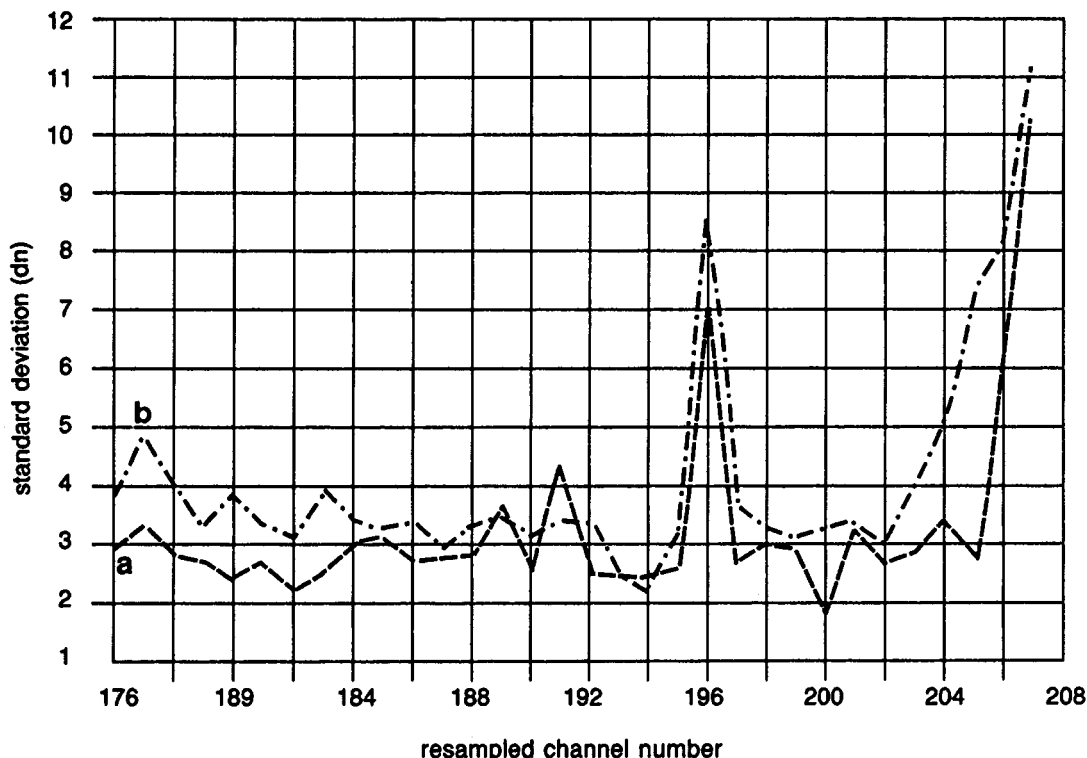


Fig. 3. Standard deviation of reflectance for spectrometer D for bright (a) and dark (b) calibration targets.

Second, the "noisy" channel (196) at 2.31 micrometers stands out clearly. Third, noise levels increase rapidly at the longer wavelengths in this range.

Signal-to-noise figures were computed based on "coefficients-of-variance" (Simpson and others, 1960) measurements of the hardpan target. Figure 4 plots the reflectance of the hardpan over relevant wavelengths as acquired by an IRIS, and these data show that the hardpan approximates a 50-percent albedo target over this spectral range. The curve reflects a fall-off in solar irradiance from 2.1 to 2.4 micrometers. Figure 5 depicts signal-to-noise estimates based on the coefficients-of-variance method. The numbers given in this plot are generally lower than published figures (Vane, 1987b), particularly at the longer wavelengths.

Data Analysis

Two approaches were used to evaluate the analytical utility of AVIRIS data. The first involved the use of standard image processing and enhancement techniques, such as band ratioing, principal components analysis, and band averaging, to generate products for visual interpretation. The second approach took advantage of spectrometric properties of the AVIRIS system using the SPectral Analysis Manager (SPAM) software (Mazer and others, 1987) to interrelate image spectra to ground measurements.

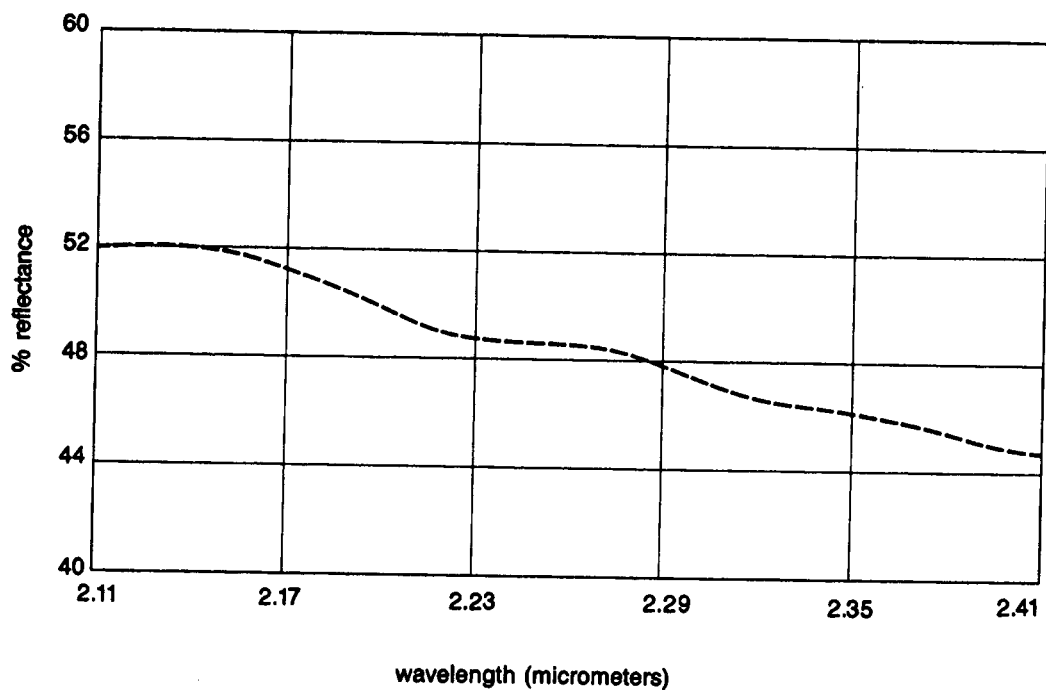


Fig. 4. Percent reflectance for a bright calibration target as measured with a field spectrometer.

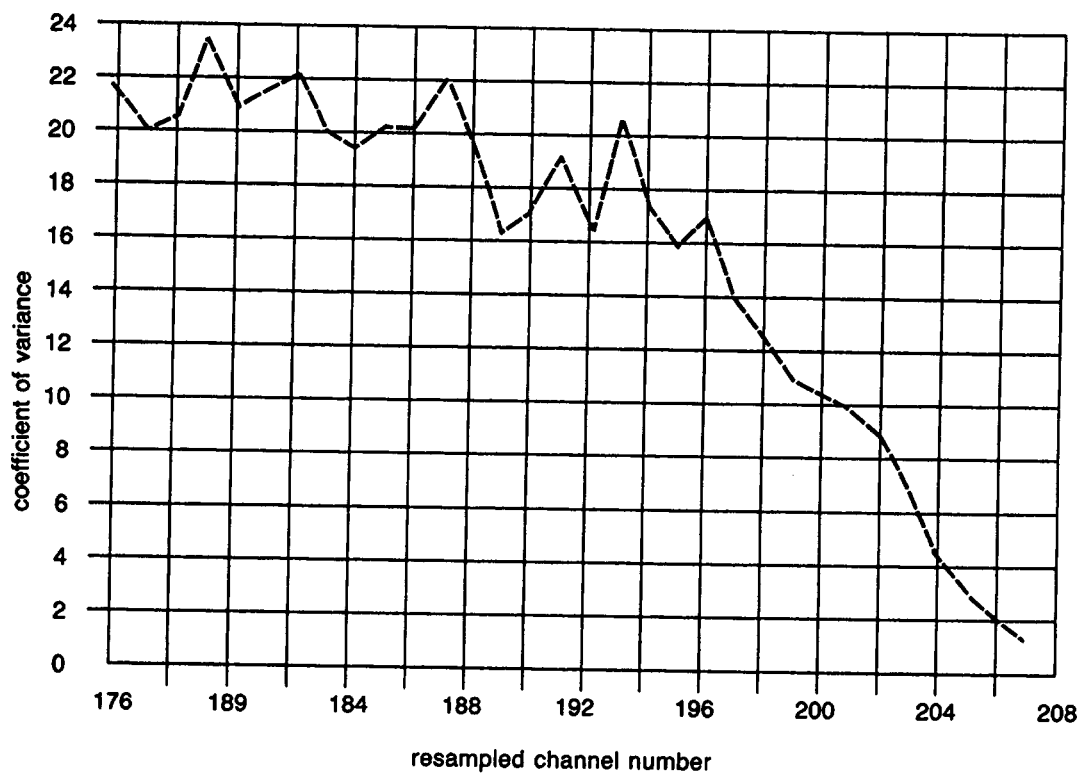


Fig. 5. Signal-to-noise ratio for 50-percent reflectance calibration target.

Criteria for determining the spectral performance of AVIRIS included the ability to discriminate iron oxide, hydroxyl-bearing, and carbonate mineral absorption features from image spectra. Thus, the analysis addressed the 0.41-0.71 (spectrometer A), 1.59-1.62 (spectrometer C), and 2.11-2.41 (spectrometer D) micrometer regions. In spite of the poor signal-to-noise characteristics of spectrometer D data, information extraction efforts focused on data from that spectrometer because of hydroxyl-bearing and carbonate mineral absorption features of interest in that region of the spectrum and because of interest in determining what effects the poor signal-to-noise characteristics had on information extraction.

Image products generated from digital processing and enhancement techniques applied to AVIRIS data were generally disappointing. In no case was an image produced that displayed the distribution of iron oxide, hydroxyl-bearing, and carbonate minerals with as good clarity and detail as displayed in similarly processed Landsat thematic mapper data of the area. These results were not surprising, however, given the measured signal-to-noise ratios of spectrometer D data. Attempts to improve the signal-to-noise by computing multiple-band averages for certain hydroxyl features in the 2.2 micrometers region met with little apparent success, and they were likewise unsuccessful for carbonate features in the 2.31-2.35 micrometers range. The latter problem likely was due to the presence of a noisy detector at 2.31 micrometers and to the generally low-albedo nature of the carbonate rocks in the Drums Mountains. Due primarily to higher signal-to-noise in the A spectrometer, good results were achieved in displaying iron oxide distribution using approximations of TM band ratio 3/1.

Results of studies to relate AVIRIS image spectra to ground and laboratory spectral measurements using SPAM software met with varying success. Matching techniques implemented within SPAM and used for data calibration in this approach included: (1) flat field corrections, (2) regression ("empirical line"), and (3) "equal energy" normalization (Conel and others, 1987). The flat field correction used the hard-pan target for reference, whereas the empirical line method used all three Pavant Butte calibration targets as points on a ground reflectance versus image digital counts regression line. The third method does not require use of an independent calibration site, but rather involves normalization of primary site target albedos to determine empirical "air-to-ground" relationships.

Several factors must be considered when analyzing data calibrated by these techniques. First, the poor signal-to-noise characteristics of the D spectrometer dictated use of spectral filtering. Figure 6 illustrates the use of the SPAM function FILTER with and without weighted averaging. Note the spectral shifts which can occur as a result of this operation. Second, the reference areas in the Pavant Butte scenes are 300 to 600 meters lower in elevation than the target areas in the Drum Mountains, which possibly affected the results from the first two methods due to different atmospheric pathlengths. Third, AVIRIS data were truncated to 8 bits for SPAM processing, although this probably had no impact on the degraded data from

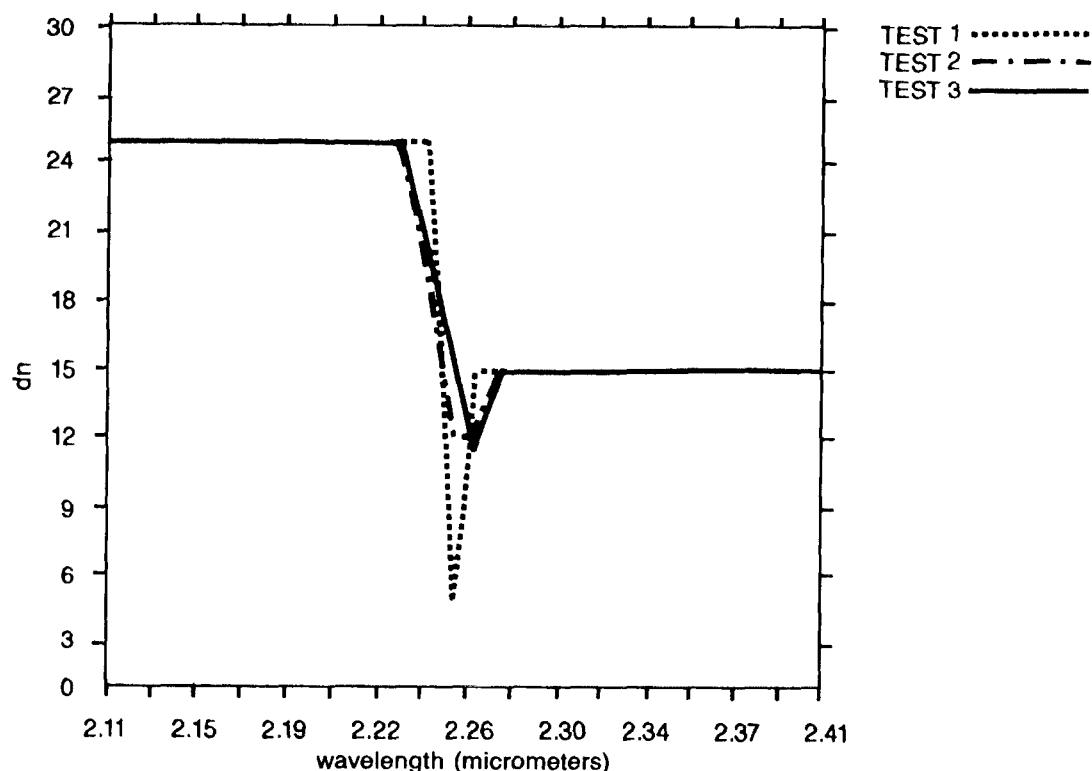


Fig. 6. Test plots of an asymmetrical spectral feature and subsequent results of the SPAM function FILTER. TEST 1 is the raw data; TEST 2 is the result from the box filter; TEST 3 is the result from the weighted filter. Filter size is 3 in both cases.

spectrometer D. Finally the empirical line technique discussed above was implemented in SPAM using several intermediate byte variables that introduced a substantial quantization error into the process.

After the data were calibrated, targets in the Drum Mountains were used to assess the instrument's ability to provide data that would resolve both hydroxyl-bearing and carbonate mineral absorption features. The altered intrusive was used as the primary hydroxyl-bearing target for analysis.

All three calibration techniques produced image spectra that resolved the major ground-measured hydroxyl features, although the width and depth of the features varied between the different techniques (fig. 7). The empirical line method did not perform as well as the other methods, probably due to the quantization error and elevation differences. In general, absorption features in the AVIRIS spectra appeared to be shifted about 10 nm toward shorter wavelengths compared to both IRIS and PIDAS spectra. Once again, due to poor signal-to-noise characteristics, different carbonate features in the 2.31-2.35 micrometer region could not be resolved.

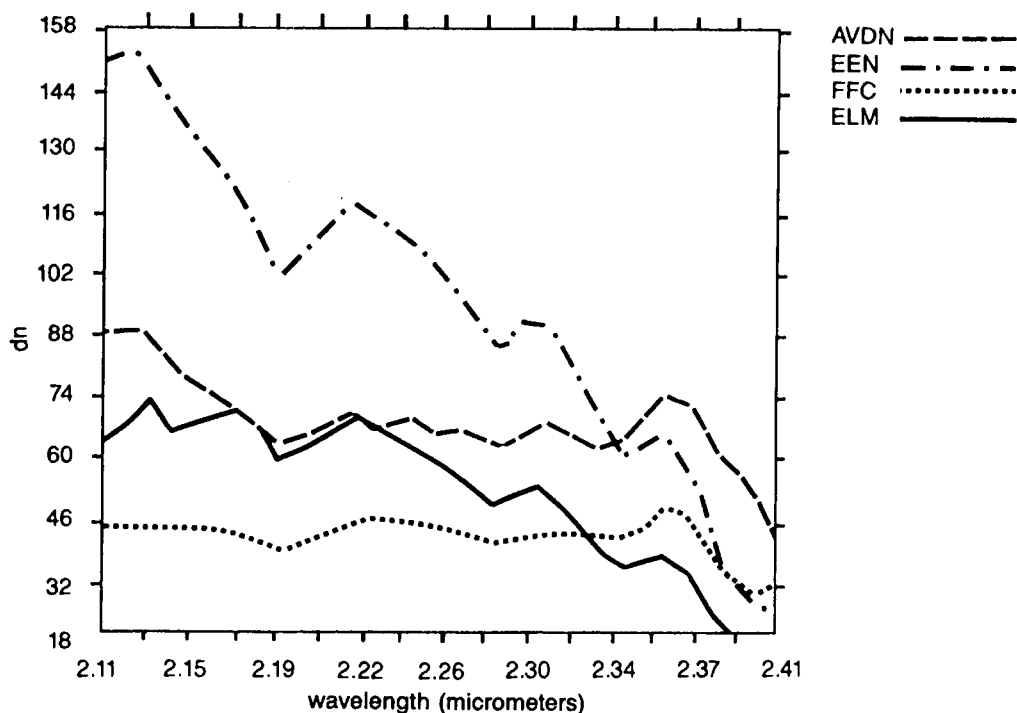


Fig. 7. AVIRIS spectral curves for altered intrusive. AVIRIS data were radiometrically corrected without spectral resampling; bad data channels were replaced; and data were spectrally smoothed in SPAM using a 3-point weighted filter. ADVN is a plot of AVIRIS DN's; EEN is derived from equal energy normalization; FFC was extracted after flat-field correction; and ELM is a preliminary result from AVIRIS data calibrated using the empirical line method.

SUMMARY AND CONCLUSIONS

These studies accomplished some, but not all, of their original objectives. The radiometric characteristics of AVIRIS data acquired over the Drum Mountains and Pavant Butte sites have been documented, and procedures used to correct detrimental artifacts in the data have been described. However, objectives related to geometric characteristics of AVIRIS are yet to be addressed.

In general, data acquired by the A and C spectrometers were of sufficiently good quality to identify iron-oxide-bearing rocks. However, poor signal-to-noise characteristics in spectrometer D limited the ability to discriminate and identify hydroxyl-bearing rocks and minerals and precluded differentiation of carbonate minerals, particularly in images of AVIRIS data. Major absorption features of hydroxyl-bearing minerals were resolved in spectra of raw,

normalized, and ground-calibrated AVIRIS data. Conclusive evaluations of AVIRIS data capabilities for lithologic discrimination and mineral identification were not possible from the data set acquired. Such evaluations should be possible following recent improvements in the signal-to-noise characteristics of spectrometer D and other repairs made to the AVIRIS system, and they will be made if a second data set is acquired over the study sites.

REFERENCES

- Bailey, G. Bryan. 1974. The occurrence, origin, and economic significance of gold-bearing jasperoids in the central Drum Mountains, Utah. Stanford University Ph.D. Dissertation, 300 pp.
- Bailey, G. B., Dwyer, J. L., and Podwysocki, M. H. 1985. Evaluation of Landsat Thematic Mapper data for geologic mapping in semi-arid terrains (abs.). In International Symposium on Remote Sensing of Environment-Remote Sensing for Exploration Geology, Fourth Thematic Conference, San Francisco, California, 1985, Proceedings (Ann Arbor, Michigan: Environmental Research Institute of Michigan), v. I, pp. 325-326.
- Conel, J. E., Green, R. O., Vane, G., Bruegge, C. J., and Alley, R. E. 1987. Airborne imaging spectrometer-2: radiometry and a comparison of methods for the recovery of ground reflectance. In Airborne Imaging Spectrometer Data Analysis Workshop, Third, Proceedings (Pasadena, California: Jet Propulsion Laboratory 87-30, August 1987), pp. 18-47.
- Lindsey, D. L. 1979. Geologic map and cross-sections of Tertiary rocks in the Thomas Range and northern Drum Mountains, Juab County, Utah. (Washington, D.C.: U.S. Geological Survey), map I-1176.
- Mazer, A. S., Martin, M., Lee, M., and Solomon, J. E. 1987. Image processing software for imaging spectrometry. In Imaging Spectroscopy II, San Diego, California, August 1987, Proceedings, ed. Gregg Vane (Bellingham, Washington: SPIE), v. 834, pp. 136-139.
- Moik, Johannes G. 1980. Digital processing of remotely sensed images. NASA SP-431, pp. 25-26.
- Reimer, J. H., Heyada, J. R., Carpenter, S. C., Deich, W. T. S., and Lee, M. 1987. AVIRIS ground data-processing system. In Imaging Spectroscopy II, San Diego, California, August 1987, Proceedings, ed. Gregg Vane (Bellingham, Washington: SPIE), v. 834, pp. 79-90.
- Simpson, G. G., Roe, A., and Lewontin, R. C. 1960. Quantitative zoology (New York: Harcourt Brace), pp. 90-143.
- Vane, Gregg. 1987a. Personal communication, January 1987.
- Vane, Gregg. 1987b. First results from the Airborne Visible/Infrared Imaging Spectrometer (AVIRIS). In Imaging Spectroscopy II, San Diego, California, August 1987, Proceedings, ed. Gregg Vane (Bellingham, Washington: SPIE), v. 834, pp. 166-174.